



This is a repository copy of *Fault-tolerant individual pitch control using adaptive sliding mode observer*.

White Rose Research Online URL for this paper:
<http://eprints.whiterose.ac.uk/138614/>

Version: Published Version

Proceedings Paper:

Liu, Y., Patton, R.J. and Lan, J. (2018) Fault-tolerant individual pitch control using adaptive sliding mode observer. In: Simani, S. and Patan, K., (eds.) IFAC-PapersOnLine. 10th IFAC Symposium on Fault Detection, Supervision and Safety for Technical Processes SAFEPROCESS 2018, 29-31 Aug 2018, Warsaw, Poland. International Federation of Automatic Control , pp. 1127-1132.

<https://doi.org/10.1016/j.ifacol.2018.09.723>

© 2018 IFAC (International Federation of Automatic Control). Reproduced in accordance with the publisher's self-archiving policy.

Reuse

Items deposited in White Rose Research Online are protected by copyright, with all rights reserved unless indicated otherwise. They may be downloaded and/or printed for private study, or other acts as permitted by national copyright laws. The publisher or other rights holders may allow further reproduction and re-use of the full text version. This is indicated by the licence information on the White Rose Research Online record for the item.

Takedown

If you consider content in White Rose Research Online to be in breach of UK law, please notify us by emailing eprints@whiterose.ac.uk including the URL of the record and the reason for the withdrawal request.



eprints@whiterose.ac.uk
<https://eprints.whiterose.ac.uk/>

Fault-tolerant Individual Pitch Control using Adaptive Sliding Mode Observer

Yanhua Liu* Ron J. Patton* Jianglin Lan**

* *School of Engineering and Computer Science, University of Hull, Cottingham Road, Hull, HU6 7RX, UK (e-mail: yanhuanyu1@163.com, r.j.patton@hull.ac.uk).*

** *Department of Automatic Control and Systems Engineering, University of Sheffield, Portobello Street, Sheffield, S1 3JD, UK (e-mail: lanjianglin@126.com).*

Abstract: Due to the increasing size of wind turbines, the unbalanced loads caused by the uneven spatial distribution of wind speed and turbulence are becoming larger and larger. As has been proved, individual pitch control (IPC) can mitigate the blade asymmetric loads greatly in region 3. On the other hand, the pitch actuator faults can affect the pitching performance with slow dynamics, resulting in generator power instability and even deteriorating the unbalanced loads of blades. However, the effects of unbalanced blade loads deterioration caused by pitch actuator faults have not been taken into account by the traditional IPC design. In the present paper, a fault-tolerant control (FTC) strategy using adaptive sliding mode estimation is combined with a traditional IPC system based on two different control methods (Proportional-Integral and H_∞ loop-shaping). It maintains the nominal pitch performance and removes the negative effects of pitch actuator faults on generator power and unbalanced blade loads perfectly. The effectiveness of the proposed strategy is verified on the 5MW NREL wind turbine system.

© 2018, IFAC (International Federation of Automatic Control) Hosting by Elsevier Ltd. All rights reserved.

Keywords: Individual pitch control, load reduction, pitch actuator faults, sliding mode observer.

1. INTRODUCTION

As a sustainable and economical renewable energy, wind energy is contributing more and more to energy supply in recent years. With increasing blade length and flexible structures, wind turbine blades suffer greatly from asymmetric loads and fatigue due to non-uniformity and turbulence of the incoming winds, which further affects the non-rotating turbine structures including hub, main bearing, nacelle and tower (Lu et al. (2015)). These structural loads can give rise to cyclic fatigue loading and shorten the lifetime of wind turbines. Moreover, large rotor wind turbines tend to be operated offshore and expensive in maintenance, this increases the demand on safety and reliability.

It has been shown that individual pitch control (IPC) can mitigate the blade fatigue effectively and prolong the wind turbine life, which has attracted significant interests on unbalanced load mitigation (Bossanyi (2003)). Various control methods, e.g. Proportional-Integral (PI) (Bossanyi (2005)), H_∞ loop-shaping (Lu et al. (2015)), Model predictive control (Mirzaei et al. (2012)), PI-R control (Zhang et al. (2014)) and different design strategies e.g. individual blade control (Han and Leithead (2014)), Coleman Transformation-based IPC (Van Engelen (2006)), feed-forward feedback control based on LIDAR (Laks et al. (2010)) are studied extensively. PI-IPC method based on Coleman transformation has been demonstrated to mitigate rotating and non-rotating loads effectively, with the

advantage of easy implementation in reality (Bossanyi (2005), Van Engelen (2006)). Moreover, a PI-IPC system developed by Garrad Hassan has been tested and verified on the CART-2 wind turbine supplied by NREL (Bossanyi and Wright (2009)). There may be faults in real pitch systems that can affect IPC performance.

It is well known that hydraulic pitch systems play a significant role in limiting the output power of wind turbines and reducing unbalanced blade loads by IPC system under high wind conditions (Lan et al. (2018)). Nevertheless, pitch systems often suffer from low pressure faults caused by oil leakage in the hydraulic supply system, resulting in slow pitch dynamics and further negative effects on operational stability and even accelerating the blade vibrations. Fault tolerant control (FTC) can compensate fault effects and maintain satisfactory system performance under faulty cases (Patton (2015)). There has been a few papers focusing on the detection and compensation of faults occurred in the pitch system. The fault detection and fault isolation (FDI) is used in the work of Sloth et al. (2011) to detect the occurrence of the actuator faults. Fault estimation (FE) observer-based FTC design has been demonstrated to be competent at obtaining the pitch actuator fault reconstruction compared with FDI (Chen et al. (2013), Shi and Patton (2015)). However, very little work has been reported to consider IPC cases, this can be a disadvantage.

The remainder of this paper is organized as follows. Two traditional IPC methods using PI and H_∞ loop-

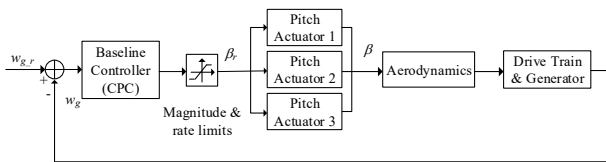


Fig. 1. Nominal pitch system scheme (CPC)

shaping are designed firstly. Meanwhile, a step-by-step sliding mode observer (SMO) (Lan et al. (2018)) is used to estimate the pitch system state and faults. Then an FE-based FTC strategy is presented to compensate the faults and recover the nominal pitch system performance and remove the effects of faults on the generator power and unbalanced loads. This work is an extension of Lan et al. (2018) which verifies the robustness and universality of the proposed FTC method in the different IPC cases and different wind conditions. The illustrative simulations are performed on the NREL 5MW wind turbine model system. Another contribution of this study is an analysis of how the occurrence of pitch actuator faults exerts an influence on the unbalanced loads, fatigue of blades, and main bearings under different IPC methods, which is seldom considered in the current research of IPC.

2. WIND TURBINE DESCRIPTION

The NREL 5MW wind turbine in Jonkman et al. (2009) is studied in this paper. FAST¹ provides a high-fidelity wind turbine with 24 degrees of freedom, which is commonly referred to as the baseline model for verifying the developed IPC algorithms (e.g. Lio et al. (2017), etc.). It is a representative commercial wind turbine with the same capacity, which does not represent any specific wind turbine in reality (Houtzager et al. (2013)).

The NREL 5MW wind turbine control strategies include generator torque and pitch controllers, from which the generator torque and pitch angle reference are produced, respectively. When the wind turbine operates in Region 2 (below rated wind speed 11.4 m/s) the generator torque controller aims at maximizing power capture and keeping pitch angles at zero to obtain full harvest of wind energy (Jonkman et al. (2009)). All the work here focuses on the above-rated wind condition (Region 3), where the primary pitch control aim is to keep the produced power around the rated value. In region 3 the case that three pitch angles are changed collectively by the same amount to regulate the generator speed is referred to as collective pitch control (CPC). If the pitch angle responds individually to the load measurements for asymmetric blade loads mitigation, this is called individual pitch control (IPC) (Lio et al. (2017)).

The CPC strategy is shown in Fig. 1. $w_{g,r}$, β_r stand for the rated values of wind turbine generator speed and three collective pitch angle, respectively. w_g , β stand for the real values. According to Jonkman et al. (2009), the pitch actuator effects are not included in FAST model. A hydraulic pitch actuator modelled as a closed-loop second-order system (Odgaard et al. (2009)) is suggested in FAST for further applications and assumed to be the same for all

¹ FAST (Fatigue, Aerodynamics, Structure and Turbulence) is a publicly available nonlinear aeroelastic wind turbine simulation code developed by National Renewable Energy Laboratory (NREL).

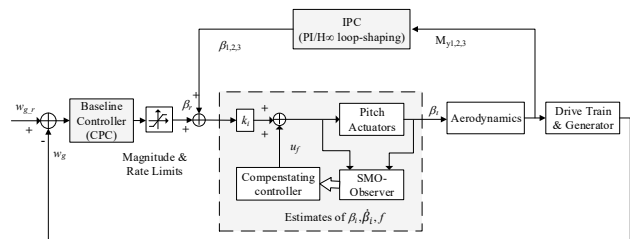


Fig. 2. Fault-tolerant pitch system

pitch systems as shown in (1). Due to real physical system constraints of actuator systems, pitch angles and rates are restricted to $[0,90]^\circ$ and $[-8,8]^\circ/s$, respectively.

$$\frac{\beta(s)}{\beta_r(s)} = \frac{w_n^2}{s^2 + 2\xi w_n s + w_n^2}. \quad (1)$$

where ξ and w_n are the nominal damping ratio and natural frequency parameters, respectively. In the fault-free cases, these parameters are considered to be equal for all the three pitch systems, with $\xi = 0.6$ and $w_n = 11.11 \text{ rad/s}$.

Due to their simplicity and ability to work under harsh conditions as well as easy maintenance, hydraulic pitch systems are widely used in large wind turbine systems. However, the pressure drop (i.e. resulting from hydraulic leakage) will cause variations in the pitch system dynamical parameters (ξ and w_n). The parameters with low pressure fault can be modelled as convex combinations of $\xi w_n, w_n^2$ and the fault level parameter f shown in (2).

$$\begin{aligned} w_n^2 &= w_{n_0}^2 + (w_{n_f}^2 - w_{n_0}^2)f, \\ \xi w_n &= \xi_0 w_{n_0} + (\xi_f w_{n_f} - \xi_0 w_{n_0})f. \end{aligned} \quad (2)$$

where ξ_0 and w_{n_0} are the nominal parameters under the normal pressure with values of 0.6 and 11.11 rad/s, respectively, while ξ_f and w_{n_f} stand for the dynamical parameters under the low pressure with values of 0.9 and 3.42 rad/s. f indicates the fault level taking values in $[0,1]$.

3. FTC-IPC SYSTEM DESIGN

The schematic diagram of FTC-IPC pitch system is shown in Fig.2, which includes the strategies of (i) a baseline pitch controller (CPC) for generator power control, (ii) an IPC system based on PI or H_∞ loop-shaping control method is designed for unbalanced blade loads reduction, (iii) SMO estimation for low pressure pitch actuator fault estimation, and (iv) FTC for fault compensation. The gain-scheduled PI pitch controller is designed as the baseline pitch controller (CPC) according to Jonkman et al. (2009).

3.1 IPC Design for Load Reduction

The objective of IPC system is to mitigate the flapwise blade bending vibrations $M_{y_{1,2,3}}$ through changing three pitch angles $\beta_{1,2,3}$ individually. A significant challenge for unbalanced load mitigation is that the three blades are rotating, which means the structural blade loads rotate with blade positions (namely azimuth angle $\varphi_{1,2,3}$) in multi-harmonics of the rotational speed resulting in a

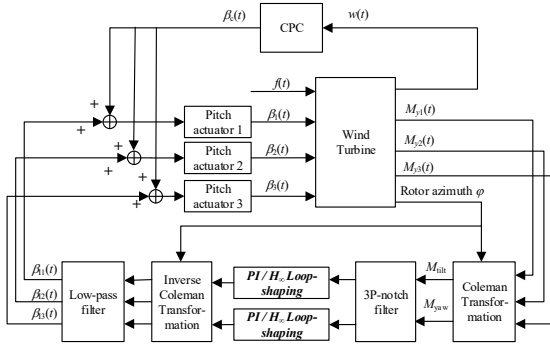


Fig. 3. The designed IPC system for load mitigation

dynamic wind loading with main rotor frequency (referred as 1P) and its multiples (2P,3P,...NP).

Coleman transformation has been used by many researchers to map three periodic flapwise bending vibrations with 120° phase difference from the blade rotational reference frame to the fixed hub reference frame (Bossanyi (2003), Van Engelen (2006), etc.). After Coleman transformation, each blade load signal is converted to a collective component which is the same for all the blades, cosine and sine (often referred to as yaw and tilt moments) components depending on the blade positions. It naturally achieves the decoupling of symmetrical (collective) and unsymmetrical (cosine and sine) blade fatigue. The main unbalanced blade loads are usually related to the unsymmetrical wind inflow conditions. As a result, the collective term is ignored for IPC. Moreover, the yaw and tilt loops can be treated as two independent channels after Coleman transformation, as the case in Bossanyi (2005). These slowly changing loads can be compensated simply and instantly by PI and other controllers. In terms of the common coordinate systems, interested readers can refer to the work in Zhang et al. (2014). Here, it should be noted that reliable sensors (i.e. strain gauges) are required for measuring the flapwise blade bending vibrations.

As the main blade fatigue comes from 1P load fluctuations, in this work the IPC system provides 1P-load mitigation. Assuming that the first blade is in the horizontal position, then Coleman and inverse Coleman transformations for 1P are given by:

$$\begin{bmatrix} M_c \\ M_s \end{bmatrix} = \begin{bmatrix} M_{yaw} \\ M_{tilt} \end{bmatrix} = \frac{2}{3} P^\top(\varphi) \begin{bmatrix} M_{y1} \\ M_{y2} \\ M_{y3} \end{bmatrix} \quad (3)$$

with

$$P(\varphi) = \begin{bmatrix} \cos(\varphi) & \sin(\varphi) \\ \cos(\varphi + \frac{2\pi}{3}) & \sin(\varphi + \frac{2\pi}{3}) \\ \cos(\varphi + \frac{4\pi}{3}) & \sin(\varphi + \frac{4\pi}{3}) \end{bmatrix} \quad (4)$$

The designed IPC system is shown in Fig.3, where f presents the inputs like wind loading and generator torque etc. As we can see, after the Coleman transformation, a simple notch filter is designed to remove the 3P-harmonic loads by avoiding the enhancement of 3P peak, which otherwise will lead to fatigue augment on the fixed wind

turbine parts. A low-pass filter with cut-off frequency of 1.2Hz is used to smooth the control signals from the designed IPC controller, which avoids the high frequency movements of pitch actuators. Firstly, the traditional PI method is adopted. The parameters of the two PI controllers are manually tuned to be the same values. The final PI-IPC controller can be illustrated in (5):

$$C_{PI-IPC}(s) = \underbrace{\frac{2}{3} P^\top(\varphi)}_{\text{Coleman}} \underbrace{\frac{s^2 + 2\xi_{n1}w_n + w_n^2}{s^2 + 2\xi_{n2}w_n + w_n^2}}_{\text{3P-notch filter}} \underbrace{\begin{bmatrix} K_p + \frac{K_{i,yaw}}{s} & 0 \\ 0 & K_p + \frac{K_{i,tilt}}{s} \end{bmatrix}}_{\text{PI controller}} \underbrace{\frac{P(\varphi)}{s^2 + 2\xi_l w_l s + w_l^2}}_{\text{Inverse Coleman}} \underbrace{w_t^2}_{\text{Low-pass filter}} \quad (5)$$

To compare the fault effects on unbalanced loads in different IPC cases, an alternative control method for designing IPC system with the same Coleman transformation-based structure is illustrated in Fig.3. To improve the system robustness, the IPC system based on H_∞ loop-shaping method in Lio et al. (2017) is adopted. The design of the H_∞ loop-shaping controller is based on the basic blade model as illustrated in the work Lio et al. (2017). Since this work focuses on the 1P load reduction, an H_∞ loop-shaping controller is designed to reduce unbalanced blade loads at the 1P frequency. The pre-compensator $W(s)$ is designed as a PI controller:

$$W(s) = K_p + \frac{K_i}{s} \quad (6)$$

The H_∞ loop-shaping controller $K_H(s)$ can then be obtained easily using a software package such as ncfsyn.m in Matlab. The final synthesised controller $K_H(s)$ is illustrated in (7). The details of the H_∞ loop-shaping controller design procedure can be found in Lio et al. (2017) and Lu et al. (2015). The proposed PI-IPC and the H_∞ loop-shaping pre-compensator parameters are shown in Table 1.

$$K_H(s) = \frac{0.00022s^5 + 0.00509s^4 + 0.06698s^3 + 0.3946s^2 + 0.8909s + 0.6623}{s^5 + 72.3s^4 + 2641s^3 + 60040s^2 + 93070s} \quad (7)$$

3.2 FTC Design for Fault Compensation

FE design The faulty pitch system based on (1) and (2) can be illustrated in

$$\begin{aligned} \dot{x}_1 &= x_2 \\ \dot{x}_2 &= G_0(x) + B_0 u + F(x) f \\ y &= x_1 \end{aligned} \quad (8)$$

where $x = [x_1 \ x_2]^\top = [\beta \ \dot{\beta}]^\top$, $G_0(x) = -w_{n0}^2 x_1 - 2\xi_0 w_{n0} x_2$, $B_0 = w_{n0}^2$ and fault distribution function $F(x) = (w_{nf}^2 - w_{nf}^2)(x_1 - u) + 2(\xi_0 w_{n0} - \xi_f w_{nf}) x_2$.

Table 1. Designed parameters

Description	Parameter	Value
PI controller (PI-IPC)		
Proportional gain	K_{pyaw}	0.00002
Proportional gain	K_{ptilt}	0.00002
Integral gain	K_{iyaw}	0.00001
Integral gain	K_{itilt}	0.00001
3P-notch filter (PI-IPC)		
Frequency	w_n	$2\pi * 0.6 \text{ rad/s}$
Damping ratio 1	ξ_{n1}	0.3
Damping ratio 2	ξ_{n2}	1
Low-pass filter (both)		
Frequency	w_l	$2\pi * 1.2 \text{ rad/s}$
Damping ratio	ξ_l	0.7
PI controller (H_∞ loop-shaping)		
Proportional gain	K_p	0.000003
Integral gain	K_i	0.000005

It can be seen that the fault distribution function $F(x)$ is time-varying, which increases the difficulty of the observer design. In this work, an adaptive step-by-step SMO proposed in Lan et al. (2018) is used to estimate the faults and the state of the pitch system as shown in (9).

$$\begin{aligned}\dot{\hat{x}}_1 &= \hat{x}_2 + v_1 \\ \dot{\hat{x}}_2 &= G_0(\hat{x}) + B_0 u + F(\hat{x})\hat{f} + v_2 \\ \dot{\hat{f}} &= \eta_f \text{sign}(e_f)\end{aligned}\quad (9)$$

where \hat{x} , \hat{f} are the state estimates and fault estimate respectively. v_1, v_2 are the SMO switching functions designed as follows:

$$v_1 = \eta_{v1} \text{sign}(e_{x1}), v_2 = \eta_{v2} \text{sign}(\tilde{x}_2 - \hat{x}_2) \quad (10)$$

where $\tilde{x}_2 = \hat{x}_2 + v_1$, $e_{x1} = x_1 - \hat{x}_1$, $e_{x2} = x_2 - \hat{x}_2$, $e_f = f - \hat{f}$, and $\eta_{v1}, \eta_{v2}, \eta_f$ are designed as:

$$\eta_{v1} = \sigma_{v1} \|e_{x1}\| + \epsilon_{v1}, \eta_{v2} = \sigma_{v2} \|e_{x2}\| + \epsilon_{v2}, \eta_f = \sigma_f \|e_f\| + \epsilon_f \quad (11)$$

where $\sigma_{v1}, \sigma_{v2}, \sigma_f$ are positive learning rates, and $\epsilon_{v1}, \epsilon_{v2}, \epsilon_f$ are small positive constants. These parameters are designed off-line and should be tuned by trial and error. Note that the symbol $\|\cdot\|$ indicates the Euclidean 2-norm.

FTC design The pitch system (8) can be rewritten as

$$\begin{aligned}\dot{x}_1 &= x_2 \\ \dot{x}_2 &= G_0(x) + w_n^2 u + F_1(x)f\end{aligned}\quad (12)$$

where $F_1(x) = (w_{n0}^2 - w_{nf}^2)x_1 + 2(\xi_0 w_{n0} - \xi_f w_{nf})x_2$.

In order to compensate the fault effect, an FTC controller is designed for the faulty pitch system (12) as

$$u = k\beta_r + u_f \quad (13)$$

where β_r is the sum of the collective pitch angle signal and the pitch angle from PI-IPC system under fault-free condition, u_f is the controller designed to compensate the actuator faults, and k is designed to modify the signal β_r .

The modification parameter k is designed as

$$k = \frac{w_{n0}^2}{\hat{w}_n^2} = \frac{w_{n0}^2}{w_{n0}^2 + (w_{nf}^2 - w_{n0}^2)\hat{f}} \quad (14)$$

The compensating controller u_f is designed as

$$u_f = -\frac{F_1(\hat{x})\hat{f}}{\hat{w}_n^2} \quad (15)$$

where $F_1(\hat{x}) = (w_{n0}^2 - w_{nf}^2)\hat{x}_1 + 2(\xi_0 w_{n0} - \xi_f w_{nf})\hat{x}_2$. The state estimates \hat{x}_1, \hat{x}_2 and fault estimate \hat{f} can be obtained

by the designed observer (9). More details about the design of the FE and FTC strategy refer to the work in Lan et al. (2018).

4. SIMULATION RESULTS

The proposed FTC-IPC design is validated on the 5MW NREL wind turbine model with simulation step 0.0125s. The wind speed input file is generated by TurbSim (Jonkman (2009)), a stochastic and full-field turbulent wind simulator software developed by NREL. The simulations are performed at 1000s above-rated wind speed, in which the mean value at hub-height is 18 m/s, together with turbulence intensity 14% and vertical shear exponent 0.2. The case when all the three pitch systems suffer from low pressure actuator faults is considered. Fault 1 occurs during the time period $t \in [200, 800]s$, and Fault 2 and 3 last for all the simulation time $t \in [0, 1000]s$. The measurement noise is modelled as a zero mean white Gaussian noise with a variance value of 1.0e-7. The designed adaptive SMO parameters for three pitch actuators are $\sigma_{v1} = 0.3, \sigma_{v2} = 0.2, \sigma_f = 0.1, \epsilon_{v1} = 0.01, \epsilon_{v2} = 0.01, \epsilon_f = 0.05$.

The simulation results are shown in Figs.4-10 and Table 2. PI-IPC and H-IPC refer to the systems including both CPC and the designed IPC based on PI or H_∞ loop-shaping method. PI-IPC-f and H-IPC-f denote the PI-IPC and H-IPC systems with three pitch actuator faults. PI-IPC-F and H-IPC-F cases represent the PI-IPC and H-IPC systems with the FTC system implemented. For the sake of simplicity, only the simulation results relating to blade 1 and the tilt moment are illustrated as follows and the results of blades 2&3 and the yaw moments are omitted. Standard deviations (STD) of the flap-wise bending moment of blade 1, the tilt/yaw moments and generator power are compared in Table 2. In addition, pitch travel ($\int_0^t |d\beta/dt| dt$) has been taken into account to approximate the damage on the pitch actuator. Fig.10 provides a direct comparison of the performances of two different IPC method both in fault-free and faulty cases. The results can be divided into three parts as follows.

First of all, the effectiveness of two IPC systems have been validated with similar vibration attenuation results on the premise of stable generator power output, which is with the cost of high pitch rate. As listed in Table 2, the pitch travel has increased impressively, by almost 350%. As we can see from Fig.10, PI-IPC performs a little bit better than H-IPC case for reducing the flapwise bending moment, tilt and yaw moment.

Secondly, the effects of the pitch actuator faults can be seen clearly. The dynamics of pitch system 1 become slow when faults occur. Moreover, due to the occurrence of other two pitch actuator faults, pitch actuator 1 still presents sluggish pitch movements even though it is fault-free. The pitch travel has increased slightly which means the occurrence of faults causes large pitch actuator motion that could lead to actuator failure. Owing to undesired fluctuations of pitch movement, the pitch angle 1 also shows more deviations resulting in enhanced imbalance of the three pitch systems. Furthermore, the generator power fluctuates more unstably as evident from Fig.7. As a result, the increasing imbalance between three pitch systems has

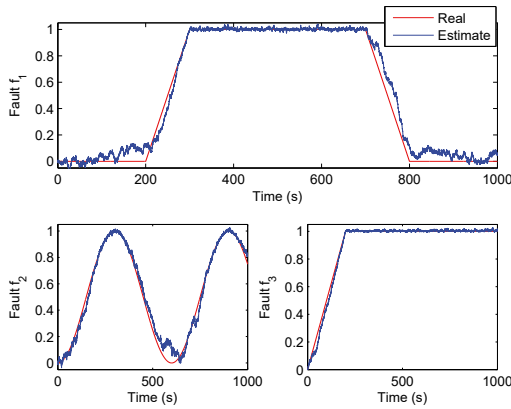


Fig. 4. Fault estimation of three pitch systems

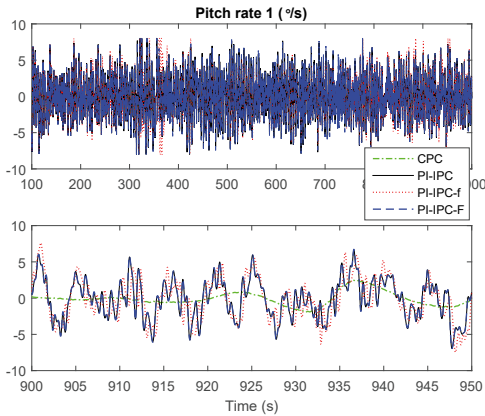


Fig. 5. Pitch rate of blade 1

magnified the asymmetric loads at the blade roots, which means the values of tilt and yaw moments grow significantly. Consequently, flapwise bending moments representing the blade fatigue have been reinforced as can be seen in Fig.8. From Table 2 and Fig.10, it can be deduced that the pitch actuator faults exert almost similar influence on blade unbalanced loads except that the PI-IPC is slightly better than H-IPC in keeping the reduction of the tilt moment.

Finally, from Fig.4 it can be seen that the three faults can be estimated very well in different IPC cases, which shows the robustness of the designed SMO. Moreover, the designed FTC strategy can restore the nominal pitch actions and compensate well the above effects caused by the pitch actuator faults. Further damage to the blade and main bearing are thus avoided, as shown in Figs.6-9. From Fig. 10, PI-IPC performs marginally better in restoring the generator power performance with the help of the proposed FTC strategy compared with the H-IPC case. Further simulations are done under other different above rated wind conditions, it could be concluded that the designed SMO parameters do not depend on the point of operation and are effective for incipient pitch actuator faults (i.e. hydraulic leakage). Hence, it can also be concluded that the tuning can be made off-line.

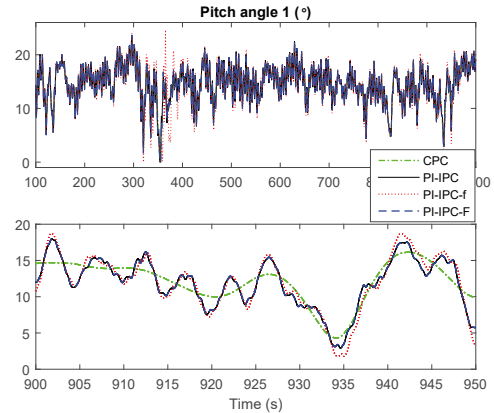


Fig. 6. Pitch angle of blade 1

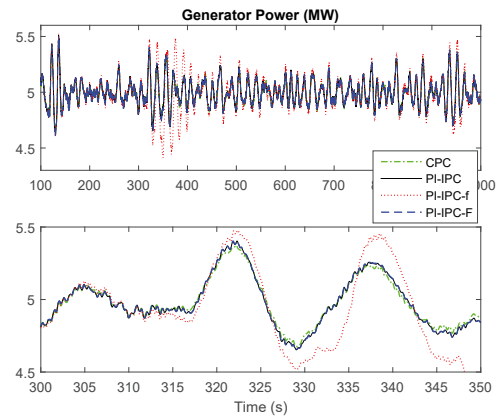


Fig. 7. Generator Power

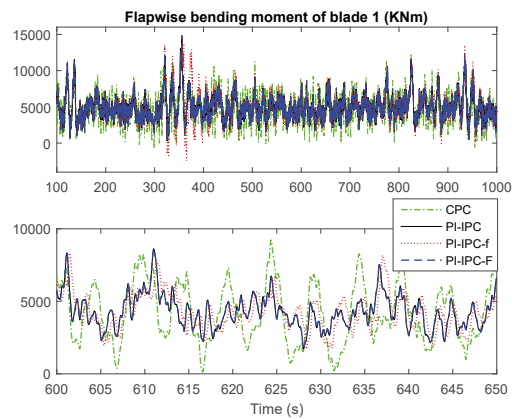


Fig. 8. Flapwise bending moment of blade 1

Table 2. Standard Deviation of Results

Parameters	CPC	PI-IPC	H-IPC	PI-IPC-f	H-IPC-f	PI-IPC-F	H-IPC-F
Flapwise (KN·m)	2286.9	1826.3	1839.4	2161.9	2188.6	1833.1	1853.5
Tilt (KN·m)	1078.4	730.8	774.1	886.2	1014.2	730.9	773.9
Yaw (KN·m)	930.7	719.7	756.6	884.4	973.7	720.2	756.0
Gen-power (MW)	129.9	134.0	132.3	168.8	168.2	134.0	132.2
Pitch travel (rad)	8.5	38.1	38.1	39.5	39.6	38.4	38.3

5. CONCLUSION

This paper analyses how and how much the unbalanced loads of blades react to the pitch actuator faults under different IPC methods, which is seldom considered in the

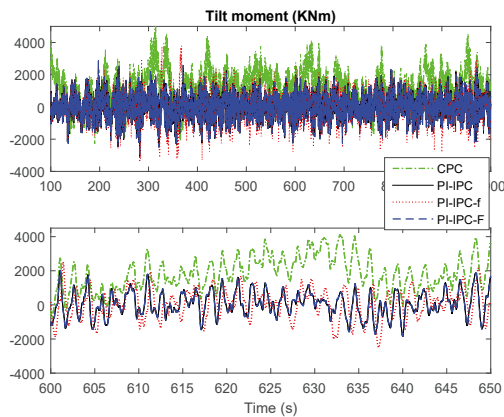


Fig. 9. Tilt moment

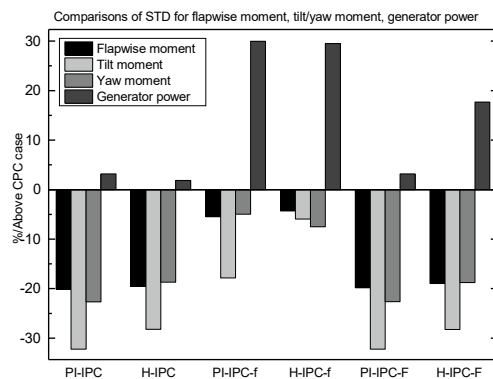


Fig. 10. Comparison result

current IPC research. From the simulation results, it can be seen that the unbalanced pitch systems caused by low pressure pitch faults indeed exert negative effects on the blade fluctuations and thus deteriorate the blade and main bearing unbalanced loads. An FTC strategy using adaptive SMO is adopted to compensate the faults in different IPC cases and observe the change of unbalanced blade loads. The proposed FTC strategy in the IPC case has been validated to achieve the objectives of maintaining nominal pitch system performance and compensating the effect to power output and asymmetric loads during pitch actuator faulty case. Combined with the former work on applying the designed FTC system to the CPC case in Lan et al. (2018), it can be deduced that the proposed FTC strategy based on the adaptive SMO could be a universal FTC structure for wind turbine systems.

6. ACKNOWLEDGEMENT

Yanhua Liu acknowledges the joint scholarship funding support from the China Scholarship Council and the Hull China Scholarship for 2015-2018. This work has been partly funded by the EPSRC Prosperity Partnership research project (EP/R004900/1) in collaboration with the Universities of Sheffield & Durham and Siemens-Gamesa, OREC and Orsted.

REFERENCES

- Bossanyi, E. and Wright, A. (2009). Field testing of individual pitch control on the nrel cart-2 wind turbine. In *European Wind Energy Conference*.
- Bossanyi, E. (2003). Individual blade pitch control for load reduction. *Wind Energy*, 6(2), 119–128.
- Bossanyi, E. (2005). Further load reductions with individual pitch control. *Wind Energy*, 8(4), 481–485.
- Chen, L., Shi, F., and Patton, R. (2013). Active ftc for hydraulic pitch system for an off-shore wind turbine. In *Control and Fault-Tolerant Systems (SysTol), 2013 Conference on*, 510–515. IEEE.
- Han, Y. and Leithead, W. (2014). Combined wind turbine fatigue and ultimate load reduction by individual blade control. In *Journal of physics: Conference series*, volume 524, 012062. IOP Publishing.
- Houtzager, I., van Wingerden, J., and Verhaegen, M. (2013). Wind turbine load reduction by rejecting the periodic load disturbances. *Wind Energy*, 16(2), 235–256.
- Jonkman, B.J. (2009). Turbsim user's guide: Version 1.50.
- Jonkman, J., Butterfield, S., Musial, W., and Scott, G. (2009). Definition of a 5-mw reference wind turbine for offshore system development. *National Renewable Energy Laboratory, Golden, CO, Technical Report No. NREL/TP-500-38060*.
- Laks, J., Pao, L.Y., Wright, A., Kelley, N., and Jonkman, B. (2010). Blade pitch control with preview wind measurements. In *Proceedings of the 48th AIAA Aerospace Sciences Meeting Including the New Horizons Forum and Aerospace Exposition*.
- Lan, J., Patton, R.J., and Zhu, X. (2018). Fault-tolerant wind turbine pitch control using adaptive sliding mode estimation. *Renewable Energy*, 116, 219–231.
- Lio, W.H., Jones, B.L., Lu, Q., and Rossiter, J. (2017). Fundamental performance similarities between individual pitch control strategies for wind turbines. *International Journal of Control*, 90(1), 37–52.
- Lu, Q., Bowyer, R., and Jones, B.L. (2015). Analysis and design of coleman transform-based individual pitch controllers for wind-turbine load reduction. *Wind Energy*, 18(8), 1451–1468.
- Mirzaei, M., Henriksen, L.C., Poulsen, N.K., Niemann, H.H., and Hansen, M.H. (2012). Individual pitch control using lidar measurements. In *Control Applications (CCA), 2012 IEEE International Conference on*, 1646–1651. IEEE.
- Odgaard, P.F., Stoustrup, J., and Kinnaert, M. (2009). Fault tolerant control of wind turbines—a benchmark model. *IFAC Proceedings Volumes*, 42(8), 155–160.
- Patton, R.J. (2015). Fault-tolerant control. *Encyclopedia of systems and control*, 422–428.
- Shi, F. and Patton, R. (2015). An active fault tolerant control approach to an offshore wind turbine model. *Renewable Energy*, 75, 788–798.
- Sloth, C., Esbensen, T., and Stoustrup, J. (2011). Robust and fault-tolerant linear parameter-varying control of wind turbines. *Mechatronics*, 21(4), 645–659.
- Van Engelen, T. (2006). Design model and load reduction assessment for multi-rotational mode individual pitch control (higher harmonics control). In *European wind energy conference*, 27–2.
- Zhang, Y., Cheng, M., and Chen, Z. (2014). Load mitigation of unbalanced wind turbines using pi-r individual pitch control. *IET Renewable Power Generation*, 9(3), 262–271.